

# Efficient Charge Recovery Method for Driving Piezoelectric Actuators with Quasi-Square Waves

Domenico Campolo, *Member, IEEE*, Metin Sitti, *Member, IEEE*, and Ronald S. Fearing, *Member, IEEE*

**Abstract**—In this paper, an efficient charge recovery method for driving piezoelectric actuators with low frequency square waves in low power applications such as mobile microrobots is investigated. Efficiency issues related to periodic mechanical work of the actuators and the relationship among the driving electronics efficiency, the piezoelectric coupling factor, and the actuator energy transmission coefficient are discussed. The proposed charge recovery method exploiting the energy transfer between an inductor and a general capacitive load is compared with existing techniques which lead to inherent inefficiencies. Charge recovery method is then applied to piezoelectric actuators, especially to bimorph ones. Unitary efficiency can theoretically be obtained for purely capacitive loads while intrinsic losses such as hysteresis necessarily lower the efficiency. In order to show the validity of the method, a prototype driving electronics consisting of an extended H-bridge is constructed for a micromechanical flying insect robot and tested by experiments and simulations. Preliminary results show that 75% of charge (i.e. more than 56% of energy) can be recovered for bending actuators such as bimorphs without any component optimization.

## I. INTRODUCTION

Piezoelectric actuators are widely used in smart structure applications due to their high bandwidth, high output force/torque, compact size, and high power density properties. As a new emerging application area, they have been utilized in mobile microrobotic applications such as micromechanical flying insects (MFI)[4], small cockroach robots [10], etc. For these robots, the overall size and weight are limited for enabling biomimetic locomotion, i.e. flying, walking, jumping, etc. Thus, there are critical limitations on the actuator and its driving electronics too. In this paper, MFI is the target application, and a compact driving electronics for piezoelectric bending actuators is aimed. The specifications of the driving electronics are quasi-square wave driving at around 150 Hz resonant frequency, weight around 20-30 mg, mechanical power output of 10 mW, and voltage source of 3-10 V using a lithium battery or microfabricated solar cells [11].

Piezoelectric actuators mostly require high input voltages. For high voltage driving, switching electronics or analog amplifiers are utilized. Since the latter would lead to excessive dissipation [8], the former is preferred. In the switching based approach, a step-up stage is first employed to generate a constant high voltage and then a half or full bridge converts

the constant high voltage into a squarewave across the load. In a step-up stage, inductors and/or transformers are used to periodically transfer electrical energy from a low voltage source to a high voltage capacitor. The rate of such a transfer, i.e. switching frequency of the step-up stage, strongly affects dimensions of inductors and/or transformers. The higher the switching rate the smaller the dimensions. A direct resonance between the parasitic capacitance of MFI actuators (10 – 20nF) and an external inductor at a frequency as low as 150Hz is thus impossible since the inductor ( $L = 220 \mu H$ ) would exceed size specifications by many orders of magnitude. Instead, a resonant high-Q LC stage, as in the case of resonant converters, shall be used to generate a high voltage oscillation when excited by a low voltage source. On the other hand, the quality factor  $Q$  of the LC circuit must be as high as the ratio of the output voltage over the input voltage, i.e.  $Q = 10 - 100$ .  $Q$  is also defined as  $Q = 2\pi E_{max}/E_{diss}$  [7] where  $E_{max}$  is the maximum energy stored in the LC oscillating circuit and  $E_{diss}$  is the energy dissipated per cycle, i.e. the energy transferred to the load at each cycle. Then, for a high  $Q$ , inductors and transformers in the LC circuit should be oversized to handle the high  $E_{max}$ . A possible remedy could consist of employing ferroelectric devices such as a piezoelectric transformer [5] whose electromechanical structure resembles an oscillating LC stage at resonance. The advantage of ferroelectric devices relies upon higher energy density compared with magnetic ones. For the MFI project, boost or flyback DC-DC converters [9] are preferred because the energy handled by the inductor (boost converter) or by the transformer (flyback) is approximately in same order of magnitude as the energy delivered to the load. Thus magnetic components need not be oversized.

After the step-up stage, a half or full bridge switching stage converts the high voltage into squarewave across the load. Due to the capacitive nature of the load, a significant amount of power is lost at any switching cycle if standard converters are employed. Therefore special care has to be taken to analyze the relationship between overall efficiency in squarewave driving and figures of merit for energy conversion of piezoelectric actuators.

Piezoelectric materials are mainly characterized by the *coupling factor* [7], which is directly related to conversion of electrical energy into mechanical one. For an actuator, not only the choice of piezoelectric material counts but another parameter is also important such as the *energy transmission coefficient*, i.e. ratio of output mechanical energy over input electrical energy [10],[14], which depends upon the geometry of the actuator, the way it is mechanically coupled to the

D. Campolo is with the University of California at Berkeley, Department of Electrical Engineering and Computer Sciences. E-mail: minmo@eecs.berkeley.edu

M. Sitti is with the Carnegie Mellon University, Department of Mechanical Engineering and the Robotics Institute. E-mail: msitti@andrew.cmu.edu

R.S. Fearing is with the University of California at Berkeley, Department of Electrical Engineering and Computer Sciences.

load and the load itself (e.g. a constant force such as gravity or a non-constant one such as a spring). Efficiency of a system is defined [13] as the ratio of the output energy over the consumed electrical energy. Although a large amount of electrical energy may be required (coupling factor) to be stored at certain time, only part of it will be transformed into mechanical work (coupling factor and energy transmission coefficient). The remainder is unused energy that can be returned to the power source [13]. As also shown in [8], part of the stored electrical energy is in fact recoverable.

In [8], recovered energy is temporarily stored in external capacitors and returned in successive cycles. As shown later such a method has intrinsic disadvantages since charging and discharging a capacitor by directly connecting it to other capacitors and/or power supplies necessarily leads to 50% energy loss even if ideal (i.e. lossless) actuators were considered. The aim of this work is to increase the efficiency when subjecting a general capacitive actuator to energy cycling by means of square wave driving. For this purpose, an external inductor is used which allows one achieving unitary efficiency at least theoretically for a purely capacitive load. Then nonideal case i.e. real piezoelectric actuators with inherent losses such as hysteresis, will also be analyzed.

For implementing the extended H-bridge, novel key elements such as an inductor for temporarily storing the energy and two diodes for self-timed switching are introduced and different from the standard H-bridges (a.k.a. full bridges in [9]), and their design principles are defined. A prototype driving stage with no component optimization is implemented and experimental results are shown.

As the outline of the paper, at first, intrinsic limits of standard charge-recovery methods are presented and then extended H-bridge based charge recovery principle for a quasi square wave case is explained. Here, the component design guidelines and the experimental results of the prototype driving stage for purely capacitive loads are given. Next, the same prototype circuit is used to drive bending type piezoelectric actuators. Differences with the previous case are emphasized and justified after a general linear model of piezoelectric electrical impedance, comprising losses, is taken into account. Finally limits to obtaining theoretical unitary efficiency are outlined from the general linear model of piezoelectric actuators.

## II. QUASI-SQUARE WAVE DRIVING METHODS

For low power piezoelectric actuation, switching output stages are preferred [8] where the losses only occur at the switching time. For this case, only two output states are available, and therefore pulse width modulation (PWM) techniques are often used [8]. In PWM systems, dissipation linearly increases with the frequency.

Switching output stages give rise to quasi-square waves voltage across the load. In Fig.(1) voltage vs. time plots and their corresponding bridge configurations both for bipolar (voltage is switched between  $\pm V_0$ ) and unipolar (voltage is switched between  $V_0$  and 0) case are shown. Piezoelectric actuators can be represented [6] as comprising a capacitor  $C$  and mechanical impedance  $Z_m$  typically characterized by

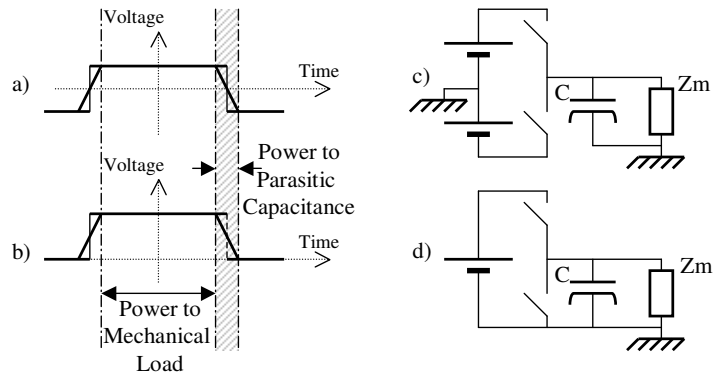


Fig. 1. Voltage vs. time plots for quasi square waves are presented both for bipolar (a) and unipolar (b) case, corresponding driving bridge schematics are shown respectively in (c) and (d) where a generally capacitive load is considered.

at least one dominant resonance frequency  $\omega_m$ , i.e. an *LRC* electrical equivalent circuit [7]. In order to excite resonance in the actuator-load system, actuators are driven by square waves at frequency  $\omega_m$ , thus during most of the time voltage is held constant performing no work on the capacitor  $C$  while transferring power to the mechanical load, only at switching time power will be dissipated by the capacitor while mechanical impedance will have small or no effect due to its slow response. Although non zero, switching time will always be negligible compared to the wave's period, corresponding to the period of mechanical resonance.

Charge recovery methods focus on reducing losses occurring at switching time, when piezoelectric actuators are mainly characterized by a (lossy) capacitive behavior, and aim to temporarily store the charge of a pre-charged capacitor before discharging it (Fig.(1)-b) or before reversing its polarity (Fig.(1)-a).

### A. Intrinsic Limits of Standard Charge Recovery Methods

Power dissipation due to periodic charging and discharging of capacitive loads has been an issue also for digital electronics technology employing CMOS logic [2],[3]. As a solution, the operating voltage level is being reduced in digital circuits. However, such a solution is not feasible for piezoelectric actuator applications where usually high stored energy is necessary. Therefore, switching circuit-based charge recovery methods aiming to temporarily store charge and later returning it (unipolar case, Fig.(1)-b) or extracting charge and immediately returning it with reversed polarity (bipolar case, Fig.(1)-a) become necessary in low power applications.

Considering a purely capacitive load, two well known facts are to be taken into account:

- Charging up an initially discharged capacitor  $C$  by means of a constant voltage source  $V$  (Fig.(2)-a) requires a total energy  $E = QV = CV^2$  that is exactly twice the final energy stored in the capacitor itself independently of switch resistance  $R$ . The final energy stored in the capacitor is thus  $\frac{1}{2}CV^2$  and the same amount has been dissipated across the resistor  $R$ .

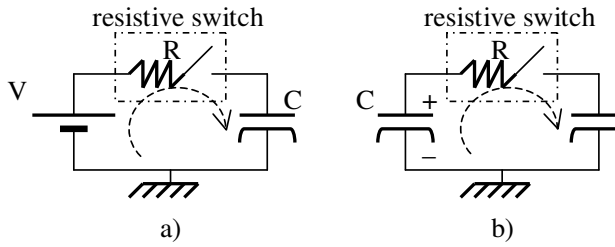


Fig. 2. (a) When charging up a capacitor by means of a constant voltage supply, the same energy is dissipated as the one eventually stored in capacitor independently of the supply intrinsic resistance. (b) Similar losses occur when two capacitors at different voltages are directly connected.

- When connecting a charged capacitor with a discharged one (Fig.(2)-b) by means of a resistive switch, the final energy will be less than the initial one depending upon the capacitors value. When  $C_1 = C_2 = C$ , which is case of interest<sup>1</sup>, the final voltage would be half of initial one, thus only 50% of charge (i.e. 25% of energy) would be recovered.

As the first point clearly suggests, directly switching a capacitive load between positive and negative constant voltage sources is *inefficient in principle* and before connecting it to a negative power supply its charge shall not be wasted but to be stored and returned later.

[8] attempts to store such an energy in another capacitor simply connecting it to the load but the second point underlines unnecessary losses arising when two capacitors are directly connected to one another.

Although reversing polarity of a pre-charged capacitor transferring its charge to a similar discharged one may solve different problems they in fact rely upon the same principle. The purpose of this work is to focus on a *natural principle* theoretically lossless, which aims to extract the whole charge from a pre-charged capacitor and use it to immediately return it with reversed polarity (bipolar fashion) or to store it in another capacitor and return it in the next cycle (unipolar fashion). Resonance, between an inductor and a capacitor, is in principle an efficient and simple way to reverse the polarity of a capacitive load. Energy is initially stored in the inductor and then returned to the capacitor with reversed polarity. Theoretically, unitary efficiency can be achieved. In the next section it will be shown how the natural resonance principle occurring in an LC parallel circuit can be exploited to recover charge.

### B. General Charge Recovery Principle for Capacitive Load

At first, the issue of reversing the polarity of a pre-charged capacitor is described.

Referring to Fig.(3)-a, for  $t < 0$  the capacitor  $C$  is to be considered pre-charged at a voltage  $V_0$  and no current  $I$  flowing in the inductor  $L$ . As soon as the switch  $S$  is turned on,

<sup>1</sup>Energy transfer is bidirectional, in case of different capacitors transfer efficiency in one direction (say  $\eta_1$ ) is advantaged at the expense of the other direction ( $\eta_2$ ). Final efficiency will be  $\eta = \eta_1 \times \eta_2$  and it is straightforward to see that only a symmetric situation (i.e.  $C_1 = C_2$ ) leads to maximizing overall efficiency  $\eta$ .

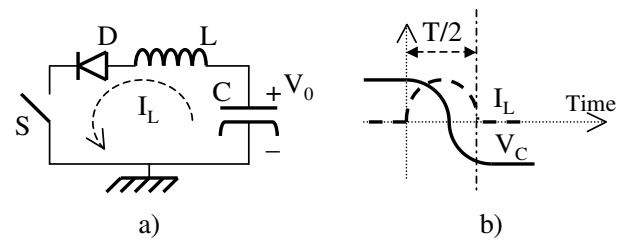


Fig. 3. (a) Circuit for reversing polarity of a pre-charged capacitor. (b) Ideal voltage across capacitor ( $V_C$ ) and current ( $I_L$ ) vs. time plots.

current will start flowing in the positive direction (shown by the arrow). Diode  $D$ , which will be at first considered ideal in order to outline the principle, will only allow current to flow in the positive direction, behaving thus as a short circuit, and will not allow negative current, in which case it will be considered disconnected.

At time  $t = 0$ , when the switch  $S$  is turned on, a positive current will start to flow and the whole circuit will behave as linear  $LC$  circuit, ideally lossless, as far as the current will be positive. From basic linear circuit theory it can be easily verified that voltage across the capacitor will be  $V_C = V_0 \cos(\omega t)$  and that current in the inductor will be  $I_L = I_0 \sin(\omega t)$ , where  $\omega = 1/\sqrt{LC}$ .

Current  $I_L$  will keep positive for the first half period ( $T/2$ ), then when  $t = T/2$  the diode will disconnect leading to constant final conditions  $I_L(T/2) = 0$  and  $V_C(T/2) = -V_0$  as sketched in Fig.(3)-b, i.e. the polarity of capacitor's voltage is eventually reversed.

Linear losses will be considered later, here it is worth noticing that a simple and effective linear circuit (resonating  $LC$  circuit) is turned into a nonlinear one by the presence of the diode which will automatically disconnect exactly when the whole of polarity has been reversed, even if the switch is still turned on. This will avoid the need for accurate timing, in fact, without any diode, the switch should be turned off at exactly half the period, failure in doing so would lead to two important losses:

- $V_C$  reaches its minimum when  $t = T/2$ , interrupting the  $LC$  oscillation before or after will cause the charge not to be incompletely recovered.
- switching at a time different from  $T/2$  means switching when current  $I_L(t)$  is not completely zero, thus leading to switching losses. Resonant converters [9] are designed to switch exactly at zero-current moments in order to minimize losses.

Now that the working principle has been outlined its application to quasi-square wave driving stages will be discussed.

### C. Application of Charge Recovery Principle to Bipolar Square Wave Switching Stages

Consider a linear lossless  $LC$  resonating circuit. The voltage across capacitor  $C$ , soon after switching, can be expressed by  $V_C(t) = V_0 \cos(\omega t)$ , after half a period voltage will be  $V_C(T/2) = V_0 \cos(\omega T/2) = V_0 \cos(\pi) = -V_0$ , i.e. reversed.

Considering linear losses, i.e. an  $RLC$  circuit, given same initial conditions as in the lossless case, the final solution will be  $V_C(t) = e^{-\frac{\omega t}{2Q}} \cos(\omega t)$  where  $Q = \omega L/R = 1/\omega RC$  is the quality factor of the circuit and comprises all kinds of linear losses ( $R$ ). A more detailed examination of such losses will be carried out below.

With dissipation, after half a cycle, the diode will still disconnect leading to final condition  $V_C(T/2) = -e^{-\frac{\pi}{2Q}} V_0 = -\eta V_0$  (where  $0 < \eta < 1$  is the charge recovery efficiency), i.e. recovery will not be complete.

Since full voltage  $-V_0$  is eventually needed, a power supply has to be employed to force the capacitor (load) to final voltage  $-V_0$ . The closer  $\eta$  is to unity the less electrical work is necessary from the power supply, it is worth noticing how so far, in order to switch from  $V_0$  to  $-\eta V_0$  no work has been done by power supply at all.

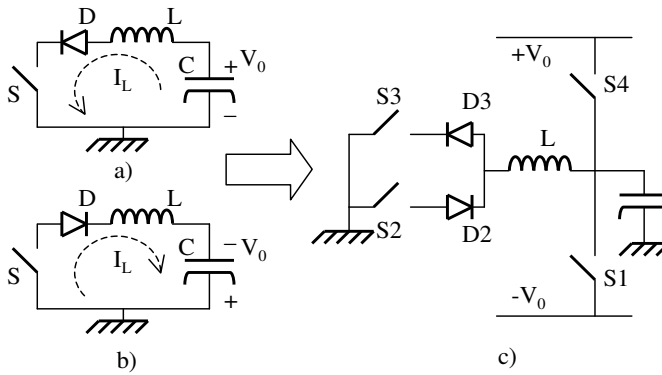


Fig. 4. Charge recovering circuits in case of a positively (a) or negative (b) pre-charged capacitor. The two circuits can merge together (c) by sharing the same inductor and with addition of two extra pre-charging switches  $S_3$  and  $S_4$ .

Fig.(4) shows how polarity of a positively (a) and negative (b) pre-charged capacitor is reversed, the two circuits only differ for the orientations of the diode. The two circuits can merge (Fig.(4)-c) to provide both transitions and the same inductor can be shared leading to reduction of size and weight which is of primary importance in applications such as [4]. Two switches ( $S_1$  and  $S_4$ ) are added to force the capacitor to the final voltage of  $V_0$  or  $-V_0$ .

#### D. Application of Charge Recovery Principle to Unipolar Square Wave Switching Stages

Although bipolar and unipolar square waves are different ways of driving a capacitive load, the charge recovery principle can be applied to both. In the unipolar case, a pre-charge capacitor should be completely discharged and, as already mentioned, in order not to lose its original charge this may be temporarily stored in another capacitor.

As shown in Fig.(5)-a, an inductor can still be used to connect a charged capacitor to a discharged one. It can easily be verified that if their capacitances are similar, in an ideal lossless situation, voltages of the charged can be completely moved from one to another as schematically depicted in Fig.(5)-b.

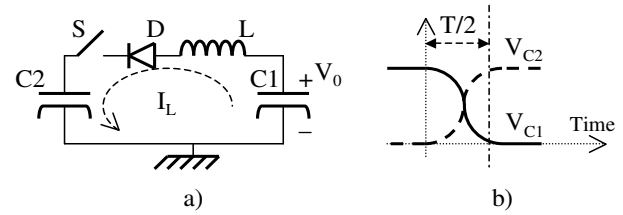


Fig. 5. (a) Charge can be transferred from a charged capacitor  $C_1$  to a discharged one  $C_2$ . (b) If  $C_1=C_2$  then the charge will be completely transferred from  $C_1$  to  $C_2$ .

It is worth to notice that it is still a resonating  $LC$  circuit where two capacitors  $C$  are in series, equivalent to a single capacitor of value  $C/2$ .

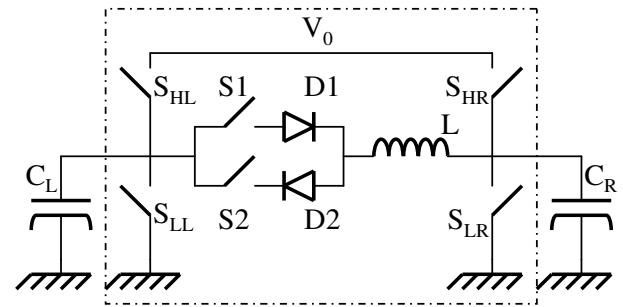


Fig. 6. Complete circuit for applying charge recovery to a unipolar square wave switching stage.  $S_{HL}$ ,  $S_{LL}$ ,  $S_{HR}$ ,  $S_{LR}$  represent a standard H-bridge.

Considering a left capacitor  $C_L$  and a right one  $C_R$ , charge can be moved from left to right or vice versa with the circuit shown in Fig.(6), where similarly to the bipolar case, two circuits are merged and extra switches are added to achieve full voltages  $V_0$  and 0 after partial ( $\eta$ ) transfer of the charge from one to another.

Referring to Fig.(6), unipolar quasi-square waves over, say, left capacitor  $C_L$  can be achieved by simply charging it up (via  $S_{HL}$ ) at first, then when it is time to discharge it, its charge can be moved and stored in  $C_R$  by means of  $S_1$  and  $D_1$ , because of non ideality not the whole of charge will be moved, that's why switch  $S_{LL}$  will be used to fully discharge  $C_L$  and switch  $S_{HR}$  to fully charge  $C_R$ , only at this moment some electrical work is required from power supply.

At beginning of the square wave's second half cycle, i.e. when it is time to recharge  $C_L$ , most of the charge can be retrieved from  $C_R$  (now fully charged) symmetrically to the way just described.

Effectiveness of the circuit depicted in Fig.(6) is mainly based on symmetry, thus it is necessary to have  $C_L = C_R$ .

Given a load characterized mainly by its parasitic capacitance  $C_0$ , a pure capacitor of value  $C_0$  can be used to match it in the aforementioned circuit. Such match may be more or less satisfactory depending upon the load.

It is very interesting to notice that both capacitors in Fig.(6) could be represented by two different loads but with similar

impedance, in such a case the two loads would match perfectly and the circuit would be still effective. Below, application of such a circuit to unimorph and bimorph actuators will be discussed.

### E. Implementation Details and Linear Losses

Prototypes for both circuits in Fig.(4)-c and Fig.(6) were realized without any attempt at component optimization but with the only aim to prove feasibility of the charge recovery principle.

All switches have been implemented by NMOS (ZVN4424) or PMOS (ZVP4424) transistors. In Fig.(4)-c, PMOS have been used for  $S_4$  and  $S_2$  while NMOS have been used for  $S_1$  and  $S_3$ , such a choice was made for sake of simplicity, in such a way every transistor would have the source pin connected to ground,  $+V_0$  or  $-V_0$  and gate voltage could easily be referred to one of these fixed voltages.

In Fig.(6), PMOS have been used for  $S_{HR}$  and  $S_{HL}$  and NMOS for all other switches. Special care must be taken with  $S_1$  and  $S_2$  since their source pin cannot be connected to ground or to  $V_0$ , therefore floating circuitry such as batteries and optocouplers has been used to drive their gate.

Both bipolar and unipolar cases rely upon a linear resonating LC circuit.

Referring to Fig.(3)-a, when diode is forward biased, i.e. in the first half period after switching, the following assumptions can be made:

- Switch can be modelled as an ideal one in series with a linear resistor  $R_S$  (ON state resistance for a MOS transistor working before saturation region).
- Diode can be modelled as an ideal one in series with linear resistor  $R_D$  and a DC source  $V_\gamma$  (typically  $V_\gamma = 0.7V$ ).
- Inductor can be modelled as an ideal one in series with a linear resistor  $R_L$
- Capacitor can be modelled as an ideal one in series with a linear resistor  $R_C$

Previous assumptions simply state that each device is working in the linear range, condition that was verified from datasheets for the prototyped circuit. Since all mentioned components are in series, their resistance can be summed up, leading to a final RLC circuit which can be analyzed with elementary linear circuit theory. Although linear, each component's resistance may be frequency dependent leading to general resistance  $R(\omega)$ , where  $\omega$  is the natural frequency.

It is convenient to consider the quality factor  $Q$  of the RLC circuit instead of its resistance and although also  $Q = Q(\omega)$  is in general frequency-varying, since an oscillating circuit is under consideration, only  $Q(\omega_0)$  is relevant, where  $\omega_0 = 1/\sqrt{LC}$ .

Such a statement needs a justification. In order to describe the behavior of the circuit in Fig.(3)-a, during the first half of a period and when real devices are employed, the equivalent linear but frequency-varying model of Fig.(7) can be deployed.

Pre-charging a capacitor is, in fact, equivalent to injecting charge into it via an ideal current source  $I_{in} = I_0\delta(t)$ , where

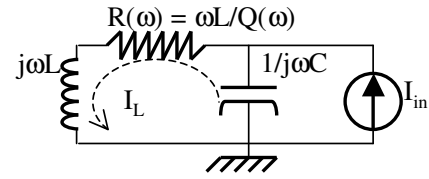


Fig. 7. An RLC linear circuit is presented where losses are frequency dependent. An ideal current source  $I_{in} = I_0\delta(t)$  is used to pre-charge the capacitor instead of a switch.

$\delta(t)$  is the Dirac pulse. This allows applying Fourier transform analysis to compute  $I_L/I_{in}$ , corresponding to transient response to pre-charging. It is clear from Fig.(7) that:

$$\frac{I_L}{I_{in}} = \frac{\frac{1}{j\omega C}}{j\omega L + R(\omega) + \frac{1}{j\omega C}} = \frac{\omega_0^2}{\omega_0^2 - \omega^2 + j\omega \frac{\omega_0}{Q(\omega)}} \quad (1)$$

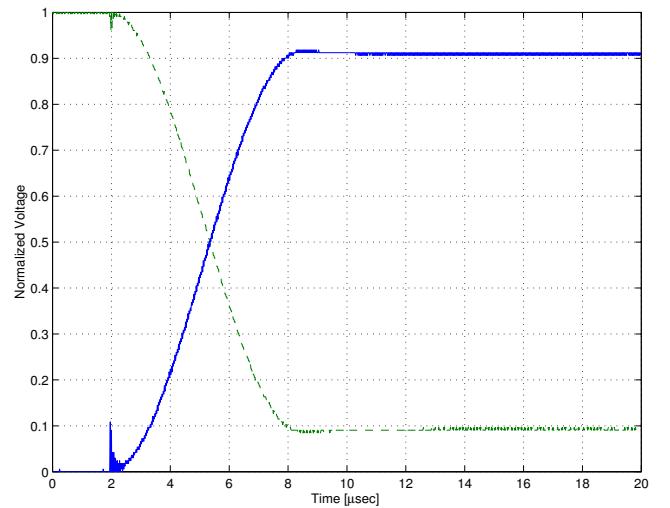


Fig. 8. Experimental data (normalized voltage across capacitors vs. time) acquired from proof of principle prototype of unipolar charge recovering circuit. More than 90% of charge is transferred, corresponding to more than 81% of energy recovery.

In Eq.(1),  $Q(\omega)$  represents the overall quality factor, i.e. comprises losses of each device (assumed to operate within the linear range).  $Q(\omega)$  can be directly evaluated from data sheets and it is straightforward verifying that the term  $j\omega \frac{\omega_0}{Q(\omega)}$ , at denominator of Eq.(1), is always negligible if compared with  $\omega_0^2 - \omega^2$  with exception of a sharp range of frequencies around  $\omega_0$  (i.e. at resonance, when  $\omega_0^2 - \omega^2 = 0$ ). Within such a range  $Q(\omega)$  can be considered constant and equal to  $Q(\omega_0)$ . Therefore only losses around the resonant frequency will mainly affect the real circuit's behavior,  $\omega_0$  has to be chosen in order to maximize  $Q(\omega_0)$ .

A further note is worthwhile, frequency dependency of  $Q(\omega)$  is mainly characterized by the inductor's  $Q_L(\omega)$ , in particular the frequencies of minimum losses. Therefore inductors have to be chosen in order to have minimum losses at the desired resonating frequency.

Previous considerations only hold if devices work within linear range; in order to verify it an upper bound of peak

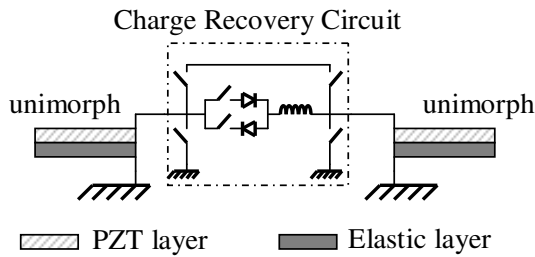


Fig. 9. Application of charge recovering unipolar circuit to a couple of similar unimorphs. Each actuator acts as a capacitor.

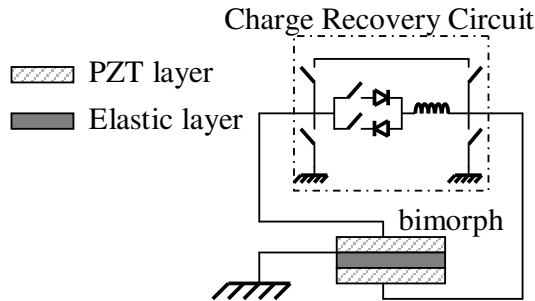


Fig. 10. Application of charge recovering unipolar circuit to a bimorph. Each half side of the actuator is meant to behave as a capacitor.

current is needed. Considering no losses (overestimation of current), the energy initially stored in the capacitor  $E_C = \frac{1}{2}CV_0^2$  will completely be transferred into the inductor at time  $t = T/4$ , i.e. the moment of peak current  $I_0$ , where  $E_L = \frac{1}{2}LI_0^2$ . By conservation of energy (no losses)  $E_C = E_L$  which easily leads to:

$$I_0 = V_0 \sqrt{\frac{C}{L}} \quad (2)$$

Such an upper bound for the peak current flowing during switching allows one to verify whether every device works in the linear range or not.

Referring to Fig.(8), normalized voltages across capacitors  $C_R = 40nF$  and  $C_L = 40nF$  of unipolar circuit in Fig soon after switching are shown and although no attempt optimization has been made, energy efficiencies higher than 80% have easily been achieved. In this particular case inductor  $L = 220\mu H$  was used and the resulting half period is:

$$\frac{T}{2} = \pi \sqrt{L \frac{C_R C_L}{C_R + C_L}} \approx 6.5 \mu sec$$

Time scale is in  $\mu sec$  while the whole square wave period is about  $6ms$  ([4] given specifications, corresponding to an insect wing beat frequency of about  $150Hz$ ) at which scale switching time is negligible, switching can thus be considered instantaneous according to the quasi-square wave assumption.

### III. APPLICATION TO PIEZOELECTRIC ACTUATORS

In this section a circuit prototype implementing charge recovery is applied to piezoelectric actuators. As already mentioned unipolar driving is more suitable to situations

where high fields are applied in order to prevent depoling of piezoelectric material. The circuit shown in Fig.(6) can be applied to similar piezoelectric actuators (unimorph, stack actuators or any kind of actuator presenting two electrodes) as shown in Fig.(9).

When actuators present more than two electrodes, such as bimorph ones, a different way of driving is also possible, as shown in Fig.(10).

A bimorph actuator can, in principle, be considered as two unimorphs bonded together. In order to avoid depoling, a single unimorph can only be driven in unipolar fashion and its resulting bending will therefore be unidirectional as well. When the charge recovery circuit drives a bimorph as in Fig.(10), only a layer at a time is driven while the other is short-circuited (zero voltage is imposed across its electrodes), behaving thus as an elastic layer. During the second half of a square wave cycle the situation is reversed, resulting in bidirectional bending.

#### A. General Linear Model For Piezoelectric Actuators

Detailed models of piezoelectric actuators have been developed during last few decades, [7] is indeed a good source for linear description of piezoelectric materials such as PZT. Whether bonded to external mechanical structures (such as cantilevers, plates, shells), clamped or freely oscillating, piezoelectric actuators can be described as a vibrating mechanical structure coupled with an electric field, acting as a generalized mechanical force [7]. Such coupling is bidirectional so that piezoelectric actuators can be modelled by linear multi-port networks, at least within certain operating ranges. One (or even more, as for bimorphs) of these ports represents an actuator's electrodes and linear network theorems can be applied in order to reduce the whole (linear) model to an electrical two-port whose impedance mirrors mechanical properties.

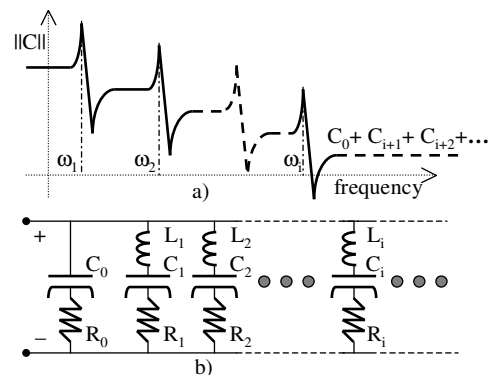


Fig. 11. Schematic diagram (a) of absolute value of generalized capacitance vs. frequency and equivalent lumped parameter description (b) for a piezoelectric actuator, each  $R_i L_i C_i$  circuit corresponds to a mechanical mode, resonating at  $\omega_i = \sqrt{L_i C_i}$ .

When dealing with a piezoelectric actuator, instead of considering its impedance  $Z(j\omega)$  (seen from the electrical port) or equivalently its admittance  $Y(j\omega)$ , it is often useful

to describe it by means of its generalized capacitance  $C(j\omega) = Y(j\omega)/j\omega$  as in [12]. A piezoelectric actuator will in fact behave as a (lossy) capacitance at almost any frequency except for sharp ranges around mode frequencies, as shown in the schematic diagram in Fig.(11)-a. An analytical description for the bimorph case can be found in [12] whose results, together with [7], can be generalized into the diagram in Fig.(11)-a.

In [7] it is also shown how to approximate the frequency-dependent behavior of Fig.(11)-a with a lumped parameter model as shown in Fig.(11)-b. Each mechanical mode is represented by an  $RLC$  circuit. Resistors  $R_i$  represent linear losses; in the general case, they are frequency dependent as well.

A main issue is whether resistors  $R_i$  can take into account any kind of losses occurring in a piezoelectric actuator, at least in the case of interest, i.e. when driven by a charge recovering circuit. Piezoelectric actuators are well known to be affected by hysteresis, which is typically a non-linear type of loss. Nonlinear models are presented in [6] for hysteresis, which is shown to occur only in the dielectric domain, i.e. it only affects electric field  $E$  and dielectric displacement  $D$  (corresponding respectively to global variables voltage  $V$  and charge  $Q$  at actuator's electrodes).

In [6], hysteresis is also shown to be rate independent, i.e. applying a periodic voltage to a piezoelectric actuator and measuring the current flowing through it leads to a voltage vs. charge plot which does not depend upon frequency of input voltage nor upon the voltage waveform (sinusoidal, saw-tooth or other), the area surrounded by the hysteresis curve is equivalent to the energy lost in a cycle. In Fig.(11)-b, dielectric domain is described by the  $R_0C_0$  branch, while any other  $R_iL_iC_i$  branch simply reflects mechanical behaviors. It is obviously impossible to perfectly describe hysteresis with linear resistors (otherwise hysteresis would be a linear phenomenon) but since the charge recovering circuit is expected to operate with currents and voltages across piezoelectric actuators resembling (half a period of) sinusoidal waveforms similarly to the pure capacitors case (Fig.(8) for  $2\mu\text{sec} < t < 8\mu\text{sec}$ ) it is still possible to determine a value for  $R_0$  such that, together with  $C_0$ , it produces losses similar to the hysteretical ones when driven at same frequency and at the same field as the actuator itself. In Fig.(12) a hysteresis plot (solid line) of a piezoelectric actuator subjected to a sinusoidal cycling voltage is shown. Here, a unimorph PZT-5H actuator is used with the given values in Table I where  $l$ ,  $w$  and  $h$  are the length, width and thickness respectively,  $E$  is the Young Modulus, and  $\epsilon$  is the dielectric permittivity. An equivalent  $RC$  circuit can be determined such that, if subjected to similar voltage input, will produce similar losses (the area surrounded by the curve itself). Capacitance is easily determined by the average slope (in a voltage vs. charge plot a pure capacitor would be represented by a straight line), while the resistance is determined after the area surrounded by the hysteresis curve is numerically computed (resistor's value is clearly frequency dependent). Both linear resistor and capacitor fitting hysteresis curve will in general depend upon maximum applied field but

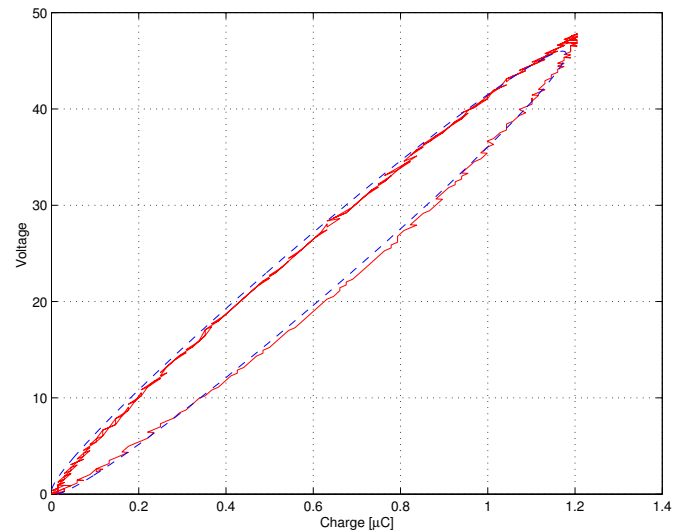


Fig. 12. Superposition of hysteresis plots (applied voltage vs. injected charge) for a piezoelectric actuator (solid line) and for a linear  $RC$  circuit (dashed line).

	$E$ (GPa)	$\epsilon$ (C/Vm)	$l$ (mm)	$w$ (mm)	$h$ ( $\mu\text{m}$ )
PZT-5H	61	$3.36 \times 10^{-8}$	16	6	127
steel	193	$\times$	16	6	76

TABLE I

PARAMETERS OF THE PZT-5H UNIMORPH ACTUATOR WITH A STEEL ELASTIC LAYER FOR THE HYSTERESIS MEASUREMENTS.

this is not an issue since the charge recovery circuit operates at a given voltage (given by square wave specifications).

So far, the applicability of linear models to the charge recovery circuit has been proved, the next section will examine results of such an application.

### B. Application Of General Linear Model For Piezoelectric Actuators To Charge Recovery Circuit

In this section, a prototype charge-recovery circuit used with piezoelectric bimorphs made out of two layers of PZT material ( $16\text{mm} \times 6\text{mm} \times 127\mu\text{m}$ ) is discussed.

Assuming as a general model the linear network in Fig.(11)-b, behavior of piezoelectric actuators can be predicted when driven by charge recovery circuit as in Fig.(9) and Fig.(10). As already mentioned, referring to Eq.(1), because of resonance between inductor (in charge recovery circuit) and load capacitance (piezoelectric actuator, in this case), only a sharp region of load impedance around the resonant frequency in fact affects waveforms during switching time (i.e. when switching diode is on,  $2\mu\text{sec} < t < 8\mu\text{sec}$  in Fig.(8)-a. Impedance at other frequencies has to be taken into account to explain behavior after switching time, i.e. soon after switching diode turns off.

Referring to Fig.(11)-a, supposing the resonant frequency  $\omega_0$  (determined by inductor and piezoelectric capacitance) to be

$\omega_i < \omega_0 < \omega_{i+1}$ , then for any mode  $n > i$  (i.e. whose resonant frequency  $\omega_n \gg \omega_0$ ), the effect of  $L_n$  can be neglected since  $\omega_0 L_n \ll 1/(\omega_0 C_n)$ , i.e.  $L_n$  can be replaced with a short circuit. Such higher modes can be simply described by an  $R_n C_n$  branch and together with  $R_0 C_0$  will determine the impedance at frequency  $\omega_0$ , thus an estimate for the capacitance of piezoelectric actuator at such frequency is:

$$\|C(j\omega_0)\| = C_0 + \sum_{n=i+1}^{\infty} C_n \quad (4)$$

which is valid when losses  $R_i$  are negligible. In the general case,  $R_0 C_0$  in parallel with  $R_n C_n$  (where  $n > i$ ) has to be considered, which is still a frequency dependent lossy capacitor.

Remaining significant modes, which are typically 3 – 5 and correspond to low frequencies  $\omega_1, \omega_2, \dots, \omega_i$ , are responsible for the oscillations arising soon after switching.

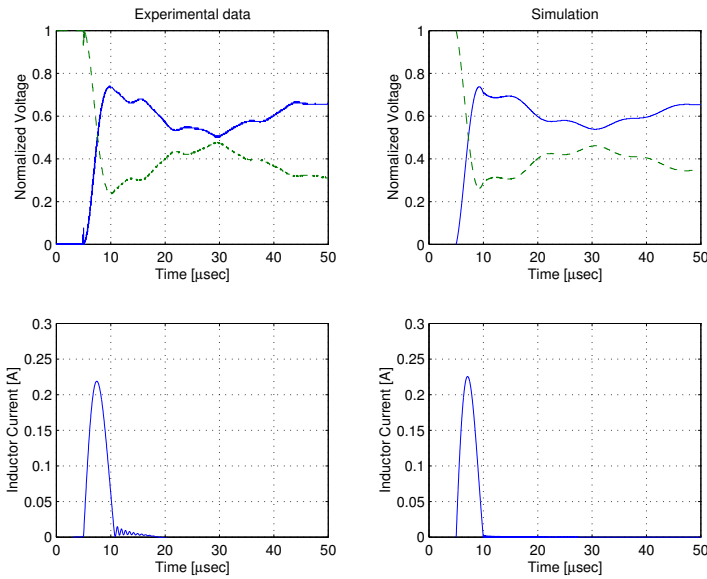


Fig. 13. Experimental normalized voltage (upper left) and current (lower left) can be compared with correspondent simulation results (upper and lower right). In this particular case a bimorph made out of two  $16 \times 6 \times 0.127 \text{ mm}^3$  PZT-5H layers was driven with  $40V$  square waves. An inductor  $L = 220\mu H$  was used in the charge-recovery circuit.

In left side of Fig.(13), the response (normalized voltage across both piezoelectric layers) of a bimorph actuator driven as in Fig.(10) is shown. At time  $t < 5 \mu\text{sec}$  one side is fully charged (dashed lines in the upper picture) and the other is fully discharged. When  $t = 5 \mu\text{sec}$ , the switch is turned on and charge between the two piezoelectric layers of bimorph actuator starts being exchanged, similarly to what happens in Fig.(8). At about  $t = 10 \mu\text{sec}$ , around 75% of charge has been transferred (i.e. recovered) and exchange between the two capacitors is over, the lower (left) picture in fact shows how current (obtained by numerically integrating voltage across inductor) can practically be considered zero after  $t = 11 \mu\text{sec}$ . At this point each side of the actuator is disconnected from the other. When real capacitors are considered, voltage is held

constant after the diode turns off (as in Fig.(8) for  $t > 8 \mu\text{sec}$ ) but when piezoelectric actuators are involved, oscillations arise. Very similar behavior can be observed when two similar unimorphs are used, as in Fig.(9), instead of a single bimorph. As an example, a model was derived in order to fit experimental results. Simulations are shown in the right side of Fig.(13). The model simply comprises an  $R_0 C_0$  ( $C_0 = 19.9 \text{ nF}$  and  $R_0 = 25\Omega$ ) branch and the first four (low frequency) modes ( $R_i L_i C_i$ ,  $i = 1, 2, 3, 4$ ) whose numerical value can be derived from Tab.II. Only modes 3 and 4 (respectively corresponding to  $\omega_3 = 2\pi \times 20KHz$  and  $\omega_4 = 2\pi \times 100KHz$ ) are visible at the displayed time scale; modes 1 and 2 are not fast enough to produce visible effects.

parameter	units	mode 1	mode 2	mode 3	mode 4
$\omega$	rad/sec	$2\pi \cdot 475$	$2\pi \cdot 2530$	$2\pi \cdot 20000$	$2\pi \cdot 100000$
$C$	nF	1.2	0.4	4	1
$Q$	-	15	30	3	10

TABLE II

SPICE parameters used to fit the behavior of the piezoelectric actuator.

The previous example was only presented to emphasize how transitions occurring during switching time are slow when compared with higher frequency modes, so that the voltage across  $C_n$  for  $n > i$  can perfectly track voltage across  $C_0$  (i.e. voltage at actuator's electrodes), but are fast when compared with remaining low frequency modes ( $\omega_1, \omega_2, \dots, \omega_i$ ) so that their effect will only take place after the switching is over. This means that the circuit will in fact only recover charge (and therefore energy) stored in capacitors  $C_0$  (which is the dominant one, representing dielectric domain) and  $C_n$  such that  $\omega_n > \omega_0$ . For capacitances associated with lower frequency modes, there will be no recovery.

A large capacitance  $C_i$ , with respect to  $C_0$ , implies a large

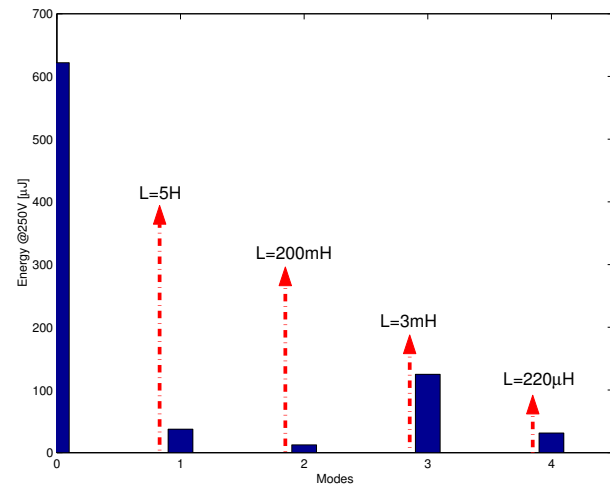


Fig. 14. Energy stored in each mode when a voltage  $V = 250V$  is applied. Vertical arrows represent, in a logarithmic scale, the inductance required to resonate at modes frequencies.

amount of energy stored in the mode  $i$ . A value for the inductor  $L$  in Fig.(6) shall be chosen in order to resonate with the piezoelectric actuator at a frequency  $\omega_0$  which is low enough to include as many modes as possible or at least the ones which store more energy. Fig.(14) shows the energy stored in each mode  $i = 1, 2, 3, 4$  (associated capacitance  $C_i$ ) and the energy stored in the electrical domain (referred to as  $i = 0$  since associated with  $C_0$ ) when a voltage  $V = 250V$  is applied<sup>2</sup>. Fig.(14) also shows the value of the inductance required to resonate at  $\omega_0 = \omega_i$ , where  $\omega_i$  represents the frequency of each mode as given in Table II.

In order to recover energy from a mode  $i$ , the inductor  $L$  must resonate at  $\omega_0 \ll \omega_i$ . From Fig.(14), it's clear how the lower  $\omega_0$  the larger  $L$  is needed. It is possible to notice an exponential growth of the required inductance. Increasing  $L$  can be a serious problem in applications where compact size and/or small weight are an issue. Size limits allow one to determine an estimate of  $\omega_0$  and, by means of an accurate model, it is possible to predict the amount of energy which is not recoverable.

#### IV. SUMMARY

In this paper a novel method for driving piezoelectric actuators with low frequency square waves for low power applications, such as micromechanical flying insect, is presented. After analyzing the relationship between piezoelectric coupling factor, actuators' energy transmission coefficient and overall efficiency, attention is focussed on the necessity of recovering electric stored energy in piezoelectric actuators for boosting efficiency. The inherent theoretical inefficiency of existing charge recovering methods, which simply transfer the load's energy directly into another capacitor, is pointed out. Alternatively, a general (i.e. valid for any capacitive load) method for charge recovery is presented which exploits highly efficient energy transfer between the capacitive load and an inductor. An implementation of such a method, where novel key components such as the aforementioned inductor, two extra switches and two self-timed turning-off diodes add charge recovery functionality to standard H-bridge topology, is tested by experiments and simulations. Without any attempt at component optimization, a proof-of-principle circuit is realized which leads to more than 92% of charge (i.e. more than 82% of energy) recovered when the load is represented by standard capacitors and more than 75% of charge (56% of energy) when real piezoelectric bimorph actuators are driven.

#### ACKNOWLEDGEMENTS

This work was funded by ONR MURI N00014-98-1-0671, ONR DURIP N00014-99-1-0720 and DARPA. Authors would like to thank all the Micromechanical Flying Insect project members for various helps.

<sup>2</sup>Operating voltage is not relevant per se since the ratio of energy stored in a mode  $i$  and the energy stored in the dielectric domain is proportional to the ratio of  $C_i$  over  $C_0$  but, especially at high fields, depending on the operating voltage the best fitting linear model may vary because of inherent nonlinearities.

#### REFERENCES

- [1] K. Agbossou, J.-L. Dion, S. Carignan, M. Abdelkrim, A. Cheriti, "Class D amplifier for a power piezoelectric load." *IEEE Transactions on Ultrasonics, Ferroelectrics and Frequency Control*, p.1036-41, vol.47, (no.4), IEEE, July 2000.
- [2] W.C. Athas, J.G. Koller, and L.J. Svensson, "An energy efficient CMOS line driver using adiabatic switching." *Proceedings of the Fourth Great Lakes Symposium on VLSI: Design Automation of High Performance VLSI Systems*, GLSV, 1994.
- [3] W.C. Athas, L.J. Svensson, J.G. Koller, N. Tzartzanis, E. Ying-Chin Chou, "Low-power digital systems based on adiabatic-switching principles," *IEEE Transactions on Very Large Scale Integration (VLSI) Systems*, pp. 398-407, vol. 2, no. 4, Dec. 1994.
- [4] R.S. Fearing, K.H. Chiang, M. Dickinson, D.L. Pick, M. Sitti, and J. Yan, "Wing Transmission for a Micromechanical Flying Insect," *Proc. of the IEEE Robotics and Automation Conf.*, pp. 1509-1515, San Francisco, CA USA, April 2000.
- [5] A.M. Flynn, S.R. Sanders, "Fundamental limits on energy transfer and circuit considerations for piezoelectric transformers," *PESC 98 Record. 29th Annual IEEE Power Electronics Specialists Conference*, p.1463-71, New York, NY, USA, IEEE, 1998.
- [6] M. Goldfarb and N. Celanovic, "Modelling Piezoelectric Stack Actuator for Control of Micromanipulation," *IEEE Control System Magazine*, vol. 17, no. 3, pp. 69-79, 1997.
- [7] H.W. Katz, ed., *Solid State Magnetic and Dielectric Devices*, John Wiley Sons, Inc., London, 1959.
- [8] J.A. Main, D.V. Newton, L. Massengill, E. Garcia, "Efficient power amplifiers for piezoelectric applications" *Smart Materials and Structures*, pp. 766-75, vol. 5, no. 6, Dec. 1996.
- [9] A.I. Pressman, *Switching power supply design*, 2nd ed. McGraw Hill, New York, 1998.
- [10] D. Ruffieux, M.A. Dubois, N.F. de Rooij, "An AlN piezoelectric microactuator array.," *Proceedings IEEE Thirteenth Annual International Conference on Micro Electro Mechanical Systems*, p.662-7, Piscataway, NJ, USA, IEEE, 2000.
- [11] M. Sitti, T. Su, D. Campolo, J. Yan, S. Avandhula, and R. Fearing, "Design, fabrication and characterization of PZT/PZN-PT unimorph actuators for micromechanical flapping mechanisms," in *Proc. of the IEEE Int. Conf. on Robotics and Automation*, Korea, May 2001.
- [12] Jan G. Smits and Arthur Ballato, "Dynamics Admittance Matrix of Piezoelectric Cantilever Bimorphs," *Journal of Microelectromechanical Systems*, pp. 105-112, vol. 3, 1994.
- [13] Kenji Uchino, *Piezoelectric actuators and ultrasonic motors*, Kluwer Academic Publishers, Boston, 1997.
- [14] Q. Wang, X. Du, B. Xu, and L. Cross, "Electromechanical coupling and output efficiency of piezoelectric bending actuators" *IEEE Trans. on Ultrasonics, Ferro. and Freq. Control*, vol. 46, pp. 638-646, May 1999.



**Domenico Campolo** received the Doctoral Degree (Diploma di Laurea) in Electrical Engineering in 1998 from the University of Pisa, Italy, and the Ph.D. degree (Diploma di Perfezionamento) in micro-Engineering from the Scuola Superiore Sant'Anna, Pisa, Italy, in 2002. During Fall 1998 he worked as a graduate student at the Department of Electrical Engineering and Communication of ZheJiang University, HangZhou, P.R. China. In 1999 he worked as a Ph.D. student at MiTech Lab, Pisa, focussing on modelling and force control issues of a piezoelectrically actuated microgripper for micromanipulation. During 2000-2001 he was a Visiting Scholar in the Department of Electrical Engineering and Computer Science of the University of California, Berkeley, where he is currently working as a Post-Doctoral Research Scholar since March 2002. His research interests mainly concern microrobotics with focus on piezoelectric actuators in low power applications, modelling and energy-efficient driving issues of resonant microelectromechanical actuators and micromanipulation.



**Metin Sitti** received the BSc and MSc degrees in Electrical and Electronic Engineering from Bogazici University, Istanbul, Turkey, in 1992 and 1994 respectively, and the PhD degree in Electrical Engineering from the University of Tokyo, Tokyo, Japan, in 1999. He worked in the CAD/CAM Robotics Department in the TUBITAK Marmara Research Center, Kocaeli, Turkey, as a research engineer during 1994-1996, working on visual servoing, computer vision, and robot control projects. He was a recipient of the Monbusho Research Fellowship during his study in Japan. He was a research scientist and lecturer at the Department of Electrical Engineering and Computer Sciences, University of California, Berkeley during 1999-2002 working on micromechanical flying insect robots and biomimetic gecko foot-hair micro/nanostructure analysis and fabrication. He is currently an assistant professor at the Department of Mechanical Engineering and the Robotics Institute, Carnegie Mellon University. His research interests include micro/nano-robotics, nanomanufacturing, biomimetic micro/nano systems, bio-nanotechnology, Scanning Probe Microscopy, haptic interfaces, and tele-robotics. He received the best paper award in the IEEE/RSJ International Conference on Intelligent Robots and Systems in 1998, and the best video award in the IEEE Robotics and Automation Conference in 2002. He is a member of IEEE, ASME, and Robotics Society of Japan.



**Ronald S. Fearing** is a professor in the Dept. of Electrical Engineering and Computer Sciences at University of California, Berkeley, which he joined in January 1988. His principle research interests are in micro robotics, tactile sensing, teletaction, and dextrous manipulation. He has a PhD from Stanford in EE (1988) and SB and SM in EECS from MIT (1983). He received the Presidential Young Investigator Award in 1991.